

Matrix metalloproteinase in the interaction between epithelial ovarian carcinoma and stromal cells: Distinct Pattern of Metalloproteinase-2 in ovarian clear cell carcinoma

Introduction:

Malignant epithelial tumors (adenocarcinomas) account for 80-90% of all malignancies of the ovary (1). Among adenocarcinomas, ovarian clear cell carcinoma (OCCA), which constitutes 5-20 % of ovarian adenocarcinoma (2,3), has been recognized as a distinct pathological subtype since 1973 (4). Patients of OCCA have worse survival than non-OCCA both at higher stages (5,6) and lower stages (7,8). However, some reported no difference in survival between OCCA and non-OCCA when tumor grade and stage were controlled (5,9,10). Other unique clinical features of OCCA include: (1) large pelvic mass, (2) rarely bilateral, (3) with endometriosis, (4) thromboembolic complication, and (5) hypercalcemia (8). OCCA was also found to have poor likelihood of response to platinum-based chemotherapy (6).

During tumor progression, invasive capacity of the malignant cells to penetrate tissue barriers for further metastases has been reported to be related to the presence of extracellular matrix-degrading proteinases, also called as matrix metalloproteinases (MMPs) (11). Overexpression of MMPs, particularly the type IV collagenase, has been demonstrated in several tumor systems and has been linked to the invasive potential of tumor cells (12-14). The most important enzyme of the MMP family in ovarian carcinoma is MMP-2 (Gelatinase A, also called type IV collagenase and 72-kDa gelatinase), which degrades basement membrane type IV collagen, as well as gelatin and type V, VII and X collagens (15). A number of naturally occurring MMP inhibitors, TIMPs 1-4, are also found in tissues (16-17). Activation of MMP-2 is blocked by TIMP-2 (18). It was reported that MMP-2 are significantly higher in malignant tumor tissues compared with their benign or premalignant counterparts (19,20), and there was a correlated elevated expression of MMP-2 with advanced tumor grade and progression (21). It is thought that the aberrant extracellular matrix (ECM) degradation in tumor biology contributes to an imbalance in local MMP and TIMP activity, resulting in the over-expression or enhanced activation of MMPs or reduced TIMP expression (22).

Interaction between MMPs and their dynamic microenvironment accounts for their activities in tumor metastasis. Ovarian tumor cells could use MMP-2 to detach from surface epithelia and migrate into the peritoneal cavity (23), and they may also use MMP-2 to invade through the basement membrane

into the ovarian stroma (24,25). Fibroblasts at the invasive edge of ovarian tumors show a striking increase in mRNA for MMP-2 and TIMP-2 (16, 26,27,28). Localization of MMP-2 either in the tumors or stromal cells has not been in consistency (2,29,30,31), and malignant ovarian tumor showed higher localization of MMP-2 in the stromal cells than benign tumors (29). So far, MMP-2 expression in OCCA was rarely reported. To establish whether OCCA is or is not biologically different in MMP activities and in the tumor cell-stromal corporation from the non-OCCA, we studied the immunohistological expression of MMP-2 and TIMP2 in various histological type of ovarian adenocarcinoma.

Material and Methods:

1. Collection of surgical specimens:

54 ovarian surgical specimens were collected during operation and then divided into two parts. One part was immediately immersed in formaldehyde and prepared as paraffin blocks. The other part was immediately stored in liquid nitrogen for zymography analysis. Clinical data of each patients were reviewed from charts from National Taiwan University Hospital.

2. Immunohistochemistry studies of extracellular matrix-degrading proteinase expression:

Serially cut, 5- μ m sections of all human ovarian tumors were immunostained using the avidin-biotin (ABC) immunoperoxidase technique (32). The sections were deparaffined with xylene and dehydrated. Hemotoxylin followed by eosin staining was first performed to identify the pathological diagnosis of the tumors. The other slides were deparaffined, dehydrated and then washed in PBSC (0.1 M phosphate buffer pH 7.4, 8.5% sucrose, 0.002% CaCl_2), incubated with 0.1% NaNO_3 and 1% H_2O_2 to remove endogenous peroxidase. 1:50 diluted normal blocking solution was added to remove any non-specific antibody bindings. Primary antibodies (MMP-2 and TIMP-2) were added and incubated overnight at 4°C. After washing with PBSC, 1:200 diluted biotin labeled second antibody was reacted for 1 hour, washed and then reacted with ABC for 30 minutes at room temperature. 0.05% DAB (*p*-diaminobenzidine-4 HCL in 0.05M Tris-HCL, pH 7.2) with 0.01% H_2O_2 was added for color development. Counterstaining using 0.01% OsO_4 was performed and the slides will then be mounted in 50% glycerol.

3. Preparation of RNA probes for in situ hybridization

(i) RNA extraction

Primary cultures from 4 to 5 different ovarian tumors were used for total RNA extraction. Total RNA was prepared according to the method of Chomczynski and Sacchi (33). Briefly, tissues or cells were homogenized with Ultraspec RNA isolation solution. The homogenate was at 4 °C for 5 min, added with 0.2 ml chloroform, and centrifuged at 12,000 xg for 15 min. The aqueous phase was added with equal volume of isopropanol and kept on ice for 10 min. The reaction mixture was centrifuged at 12,000 xg for 10 min. The pelleted RNA was washed twice with 75% ethanol and precipitated by subsequent centrifugation (75,00 xg for 5 min). The pellet was briefly dried and dissolved in DEPC-treated water. To avoid DNA contamination, total RNA was further treated with DNase I (10 unit) in the presence of RNase inhibitor (20 unit) for 30 min at 37 °C. After phenol/chloroform (3:1, v/v) extraction, the aqueous phase was recovered by centrifugation (12,000 xg for 15 min). It was then added with 1/10 volume of 2.5 M sodium acetate and 2 volume of 95% ethanol. The mixed solution was kept in a freezer (-20 °C) for at least 2 hr and centrifuged at 12,000 xg for 10 min. The pellet was then washed with 75% ethanol and dried. RNA pellet was dissolved in DEPC-H₂O and the concentration was determined by spectrophotometry.

(ii) Reverse transcription (RT)

2 μ g of the total RNA with 1 μ g/ μ l of oligo (dT) 15 primer was added to 20 μ l of diethylpyrocarbonate (DEPC) treated water, heated to 72°C for 10 minutes and then cooled in ice. 10 μ l of 5 x M-MLC buffer [50mM diethiotheritol, 375 mM KCL, 15 mM MgCl in 250 mMM Tris-HCL (pH 8.3)], 0.5 mM dNTP, 39 U RNasin, 200 U M-MLV, RNase H minus reverse transcriptase and DEPC treated water up to a volume of 50 μ l was added and bath at 42 °C for 40 minutes. The reaction was stopped at 72 °C for 10 minutes and then cooled on ice.

(iii) Polymerase chain reaction (PCR)

About 1-2 μ l of RT product was added into the PCR buffer (to a final concentration of 1.25 mM dNTPs, 10 mM Tris-HCL, pH 8.3, 50 mM KCL, and 0.1% Triton X-100), 0.5 μ M primers of MMP2 (sense:

GGGGCCTCTCCTGGACATT antisense:
TCACAGTCCGCCAAATGAA) or TIMP-2 (sense:
GGTCTCGCTGGACGTTGGAG, antisense:
GGAGCCGTCACCTTCTCTTG). 1.5 mM MgCl₂, 2 μl Tag polymerase
(Promega) to a final volume of 25 μl. After adding 50 μl of
mineral oil, PCR was performed using the program of touch down:
initial cycle as 95°C for 3 minutes, 65°C for 1 minute and 72°C for 1
minute. Second cycle as 95°C for 30 seconds, 64°C for 1 minute and 72
°C for 1 minute. The subsequent annealing temperature was dropped
by 1°C for every 2 cycles until 56°C, then continuous at 95°C for 30
seconds, 55°C for 1 minute, and 72°C for 1 minutes for 15 cycles. The
final yield was kept at 4°C. 10 μl of the final product was checked
with electrophoresis using 2% agarose gel. The PCR product was
around 150 nucleotides in size.

(iv) DNA extraction from agarose gel and sequencing

A small well was cut at the center of a 2% agarose gel and 1 μl of
PCR product was loaded. When the DNA band was at the margin of
the cut well, electrophoresis was shut off every 10 seconds and the
DNA product was yield form the TBE solution loaded into the cut well.
Phenol to a volume of 1:1 was added to remove debris and then DNA
was precipitated by adding 1/10 volume of 3M NaOAC, pH 5.2. and 2
to 2.5 volume of alcohol. The precipitated DNA was washed by 70%
alcohol, air dried, and then dissolved in TE buffer (60 mM Tris, 1 mM
EDTA, pH 8.0). The yield DNA was sent for sequencing.

(v) Cloning and transformation

0.5 to 2 μl of PCR product of the length of 150 bp was mixed with 1
μl of 3.9 kb TOPO vector to a final volume of 5 μl and incubated at
room temperature for 5 minutes. 2 μl of 0.5 M β-mercaptoethanol
with competent cells was then added and mixed gentle, incubated on
ice for 30 minutes. The cells was heat shocked for 30 seconds at 42
°C and then transferred to ice for 2 minutes. 250 μl of SOC medium
will be added and shacked horizontally at 37°C for 30 minutes. Finally
the SOC medium with the component cells and vectors was spread
on plates containing LB agarose and incubate overnight at 37°C.

(vi) Selection of colonies

50 μ g/ml of ampicillin, 40 μ l of 40 mg/mL X-Gal and 40 μ l of 100mM IPTG was added to each LB agarose plates. 10 white colonies was selected and then incubated in LB broth.

(vii) Minipreparation of plasmid DNA

After incubation, 1.5 ml of component cells was precipitated and resuspended in 150 μ l of solution I (50 mM glucose, 25 mM Tris-HCL, pH 8.0, 10mM EDTA, pH 8.0, 300 μ l) of freshly prepared solution II (0.2N NaOH, 1% SDS) was added followed by 225 μ l of solution III (3M potassium acetate, 11.5% glacial acetic acid) to lysate the bacteria. Supernatant was recovered after centrifugation and the plasmid DNA was precipitated by 2 volumes of ethanol. It was washed with 70% ethanol, air dried and dissolved in water.

(viii) Selection of the plasmid DNA with correct insert

1 μ l of the plasmid DNA was digested with restriction enzyme EcoR1 at 37 $^{\circ}$ C for 20 minutes and then checked with 2% agarose gel electrophoresis. Alternatively, using primers of SP6 promoter and t7 promoter, the sequence of the plasmid DNA, especially at the locus of insertion, was sequenced.

(ix) Large scale preparation for plasmid extraction

The component cells with the correct vector and insertion was incubated in 250 ml LB broth at 37 $^{\circ}$ C for 8 to 10 hours. Bacteria was collected when OD₆₀₀ are 0.6, centrifuged at 3500 rpm at 4 $^{\circ}$ C for 10 minutes. The pellet was resuspended in 25 μ l of solution I (described in vii), then in solution II to destroy the cell walls, and finally in solution III to precipitate the DNA component cell DNA. The supernatant was added to 0.6 volume of isopropanol for precipitation and then, the pellet was dissolved in 1 ml TE buffer (10 mM Tris, 1 mM EDTA, pH 8.0). The supernatant was added to 2 volume of pure alcohol for plasmid DNA precipitation. The pellet DNA was washed with 70% ethanol, air dried and then dissolved in TE buffer RNaseA was added and an equal volume of phenol/chloroform/isoamylalcohol (25:24:1) was used to purify the plasmid DNA. The purified plasmid DNA was then precipitated in ethanol.

(x) RNA labeling

Using SP6 and T7 promoter, the RNA labeling kit (Boehringer Mannheim) was used to dig-label the sense and the antisense of MMP-2 and TIMP-2 RNA probes. 1 μ g of the plasmid DNA was served as template and added to 2 units of either SP6 polymerase or T7 polymerase with 2 μ l of NTP labeling mixture and 2 μ l of transcription buffer to a final volume of 15 μ l. 1 μ l of RNase inhibitor was added, centrifuged and incubated for 2 hours at 37 $^{\circ}$ C. 2 μ l of EDTA 0.2 M, pH 8.0 was added to stop the reaction and the labeled RNA was precipitated with 2.5 μ l of 4 M LiCl, and 75 μ l prechilled (-20 $^{\circ}$ C) ethanol at -20 $^{\circ}$ C for 2 hours. The pellet was washed with cold 70% ethanol, dried and then dissolved in DEPC treated water. 1 μ l of RNase-inhibitor was added to inhibit any possible contaminating RNase.

(xi) Detection of Dig-labeled MMP-2 and TIMP-2 sense and antisense RNA probe

The labeled probe was serially diluted and dot blotted to the nylon paper. 0.5 J/cm² UV light was used to cross link the DNA to the nylon paper, and then the nylon paper was dried in the oven at 55 $^{\circ}$ C. The nylon paper was rinsed briefly in buffer I (maleic acid 0.1M, NaCl 0.15 M, pH 7.5, Tween 20, 0.3 % volume) and then incubated in blocking solution for 30 minutes, in 1:5000 anti-dig-AP conjugate for another 30 minutes. The paper was washed twice in buffer I and then equilibrium in detection buffer (0.1M Tris-HCl, 0.1M NaCl, 59 mM MgCl₂, pH 9.5). Color was developed in freshly prepared color solution (3.5 μ l NBT and 3 μ l X-phosphate in 1 ml detection buffer) in sealed bag without shaking. Reaction was stopped by washing with water.

4. In situ hybridization (ISH) of MMP-2 and TIMP-2 mRNA

Serially cut 5 μ m sections of all human ovarian tumors were deparaffined with xylene, rehydrated and then ISH was performed as described in previous study (32). 1 mg/ml of proteinase K was added at 37 $^{\circ}$ C for 30 minutes, and then acetylation at room temperature. The slides were then washed in PBS (phosphate saline buffer 0.1M, NaH₂PO₄, 0.1 M Na₂PO₄, 0.15 M NaCl). Prehybridization solution (50% deionized formamide, 250 μ g/ml salmon sperm DNA, 0.05% SDS, 1 x Denhart's solution, 4 x SSC, 50 mM sodium phosphate buffer, pH 6.5) was added and heated to 95 $^{\circ}$ C for 5 minutes to

denature the DNA in cells. The slides were chilled in ice and then hybridization buffer containing 0.1 μ g of dig labeled probe was added and incubated at 42 °C for overnight. After hybridization, the slides were washed sequentially with 4xSSC, 2xSSC, 1xSSC and 0.5xSSC. 10% blocking solution was first added and then 1% blocking solution containing AP linked antibodies (1:500) was added and incubated at 4 °C overnight. Maleic acid buffer was added following by detection buffer. Color development with NBT and X-phosphate was performed. The slides were mounted and examined under microscope.

5. Zymography analysis of the proteinase activities (34):

Zymography was used to identify the activity of metalloproteinase in the ovarian carcinoma. The ovarian tissue was grinded on ice and the protein was extracted. Activities of MMPs were detected by zymography, using SDS-7% polyacrylamide gels copolymerized with 1 mg/mL gelatin. Protein concentrations were measured, and equal amounts of samples were homogenized in sample buffer and directly electrophoresed. The gel was washed twice at room temperature for 10 minutes in 2.5% Triton X-100 and for 20 minutes in water and incubated overnight at 37°C in 50 mmol/l tris-HCL, pH 8, containing 5 mmol/L CaCl₂ and 1 μ mol/L ZnCl₂. Gels were stained in 30% methanol/10% acetic acid containing 0.5% Coomassie Brilliant Blue G250. Both proenzyme and active proteinase forms were detected as clear bands and analyzed by densitometric scanning using a computer-assisted analysis.

6. Heterotransplantation:

1 to 5 X 10⁷ cells of OVTW59 subclones P0 and P4 were transplanted subcutaneously into the back of 6-8 weeks old scid mice (5 for each groups). Sizes of tumor growth were recorded weekly, and when the tumors were big enough, they were removed and the mice were autopsied for metastasis. Tumors were prepared for paraffin blocks, stored in liquid nitrogen for zymography analysis.

Results:

1. Clinical Data of ovarian specimens.

Fifty cases of epithelial ovarian adenocarcinoma tissues (20 clear cell carcinoma, 15 serous papillary adenocarcinoma, 4 mucinous adenocarcinoma, 5 endometrioid adenocarcinoma, and 2 anaplastic

carcinoma, 2 recurrent ovarian adenocarcinoma after chemotherapy) and 4 cases of metastatic ovarian carcinoma (2 from breast cancer and 2 from gastric cancer) were obtained and analysed. The average age of women having clear cell carcinoma was 47.9 ± 10.7 years old, serous papillary adenocarcinoma was 56.3 ± 11.4 years old, mucinous and endometriod adenocarcinoma was 52.3 ± 12.3 years old (Table1).

Table 1. Clinical characteristic of patients with ovarian adenocarcinoma.

Tumor type	FIGO stage	Case No	Tumor size (cm)	Outcome	Recurrence
Clear cell carcinoma	I	9	15.5 ± 7.4	6N2P1E	4
Clear cell carcinoma	II	5	15.2 ± 6.5	2N1P2E	4
Clear cell carcinoma	III	6	11.8 ± 6.7	1N5E	5
Serous papillary	I	2	10,10	2N	1
Serous papillary	III	13	7.8 ± 6.7	3N10E	13
Mucinous	I	2	30,30	2N	1
Mucinous	III	2	20,9	N60	2
Endometriod	I	1	14	1N	
Endometriod	III	4	8.3 ± 7.2	4E	4
Anaplastic	III	2	20, frozen	2E	2
Recurrence	III	2	3, frozen	1E1P	2
(1 papillary, 1 clear)					
Metastatic		4		4E	

N:NED

P:Persistent

E:Expired

2. Immunohistochemical and in situ hybridization patterns of MMP-2 and TIMP-2 in ovarian tumors.

Expression of MMP-2 and TIMP-2 were mainly localized to the tumor tissue of clear cell carcinoma (Fig 1), but mainly at both the stromal and tumor tissue of other types of ovarian adenocarcinoma (Fig 2 endometriod adenocarcinoma, Fig 3: mucinous adenocarcinoma, and Fig 4: serous papillary adenocarcinoma). The distribution of MMP-2 and TIMP2 ISH was parallel to their immunohistochemical distribution. The distribution of MMP-2 in stroma and tumor tissues was showed in Fig 5 between OCCA and non-OCCAs.

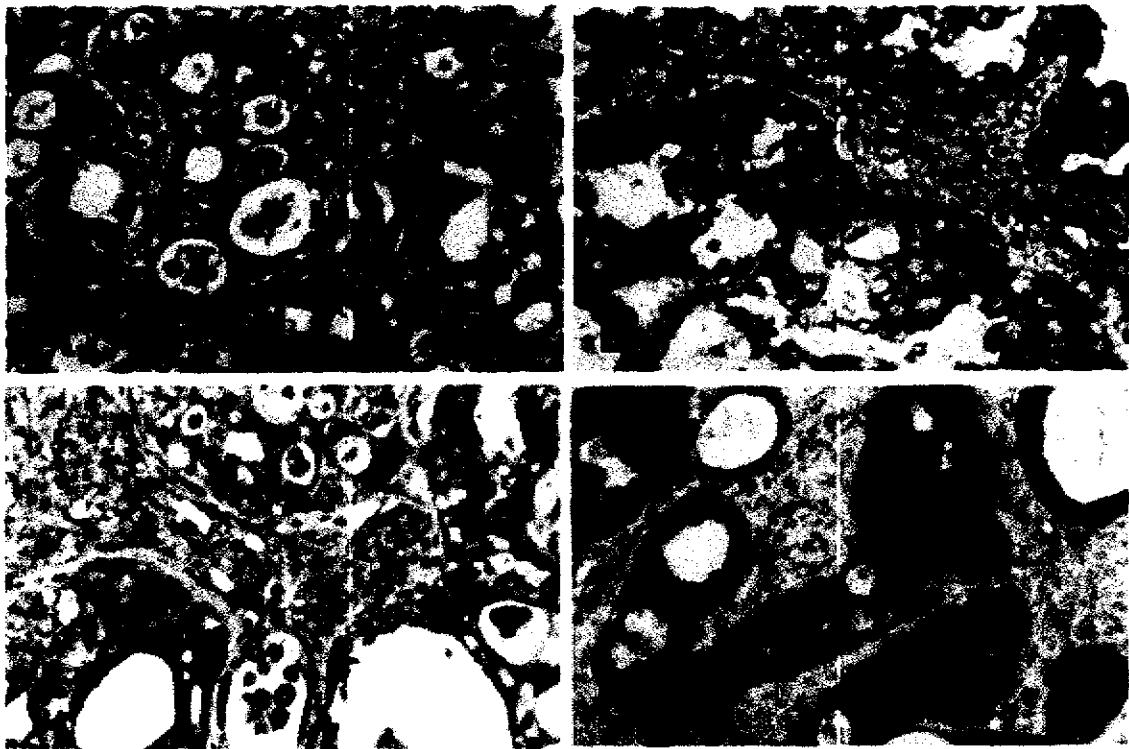


Fig 1. Immunostaining and in situ hybridization for MMP-2 (A and B) and TIMP-2 (C and D) in Ovarian clear cell carcinoma (OCCA). Both MMP-2 and TIMP-2 protein and mRNA were distributed in tumor cells (original magnification x 200).

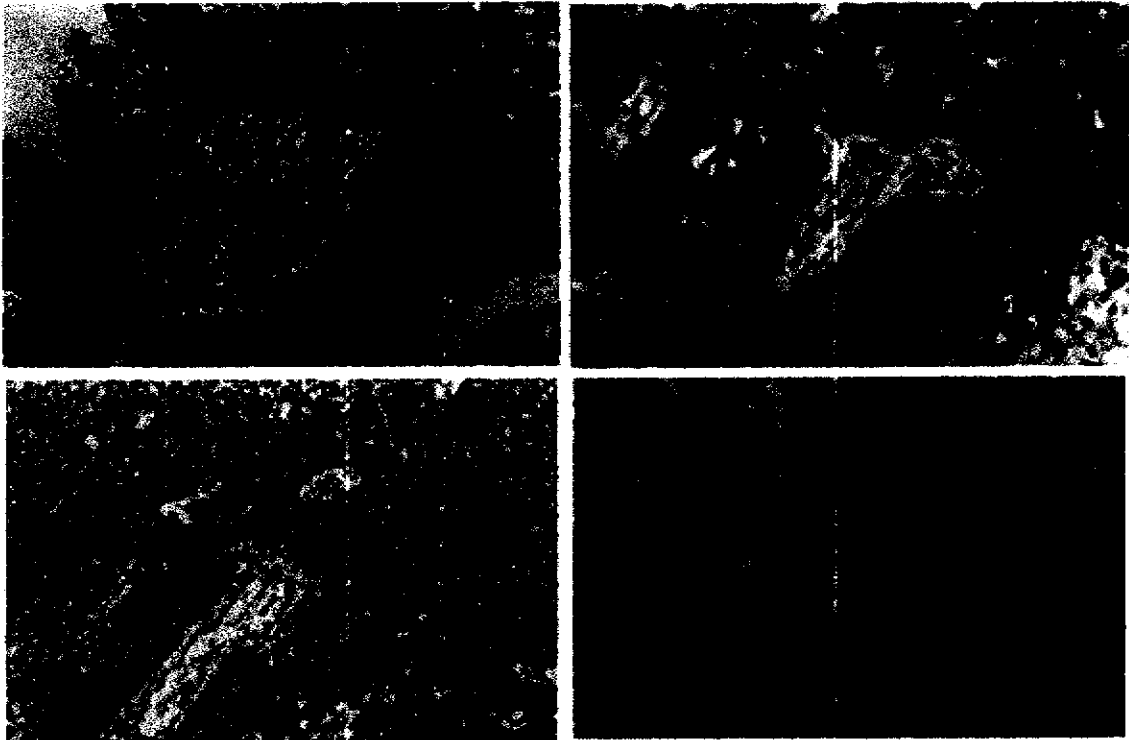


Fig 2. Immunostaining and in situ hybridization for MMP-2 (A and B) and TIMP-2 (C and D) in a case of endometrioid adenocarcinoma. MMP-2 was equally distributed in tumor and stromal cells. Distribution of TIMP-2 protein and mRNA were mainly in the tumor cells (original magnification x100)

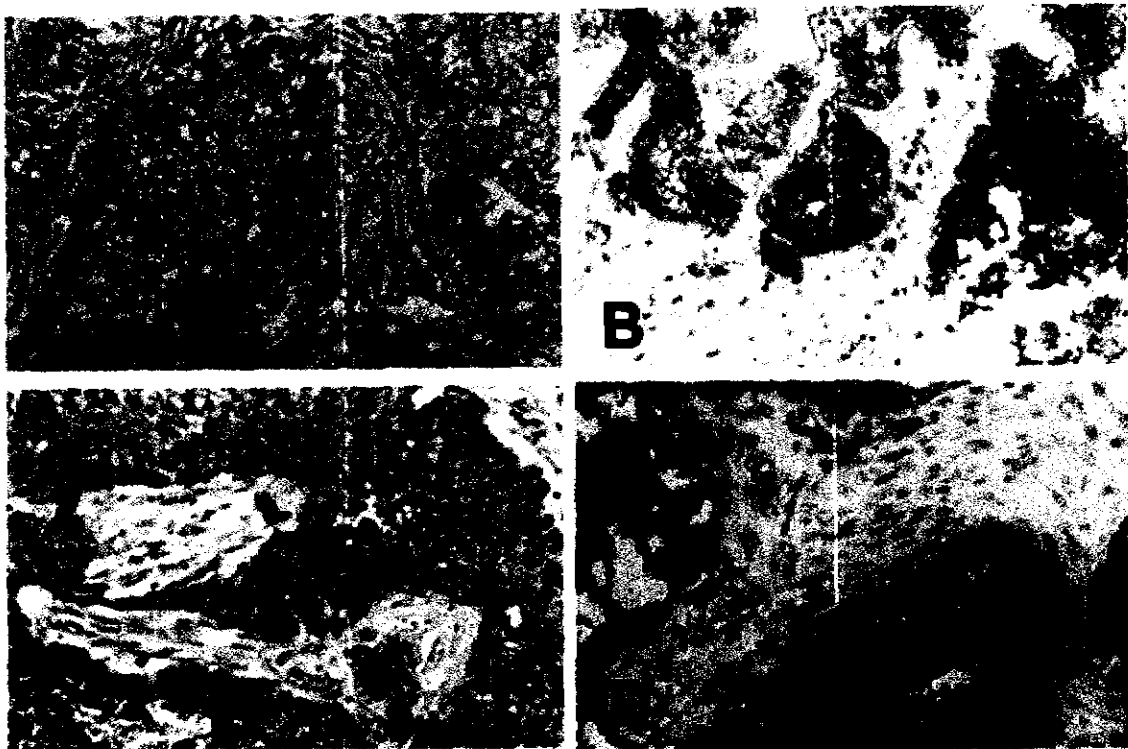


Fig 3. Immunostaining and in situ hybridization for MMP-2 (A and B) and TIMP-2 (C and D) in a case of mucinous adenocarcinoma. MMP2 protein was mainly localized at the stromal cells, and tumor cells were slightly weakly stained. TIMP-2 protein was localized more at the tumor cells than stromal cells. Both MMP-2 and TIMP-2 mRNA were equally distributed in the tumor and stromal cells (original magnification x100).

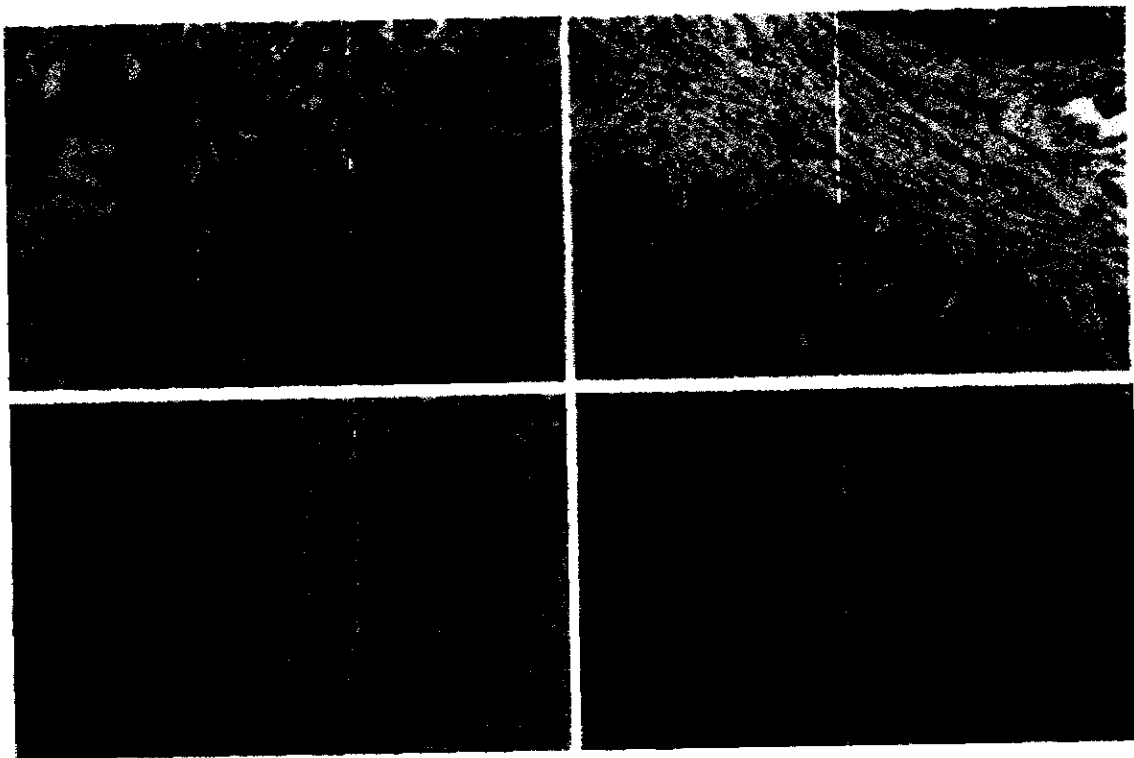


Fig 4. Immunostaining and in situ hybridization for MMP-2 (A and B) and TIMP-2 (C and D) in a case of serous papillary carcinoma. MMP2 protein was mainly localized at the stromal cells, and tumor cells were slightly weakly stained. TIMP-2 protein was weakly stained and localized more at the tumor cells. MMP-2 mRNA was equally distributed in tumor and stromal cells, TIMP-2 mRNA was found mainly at the tumor cells (original magnification x100).

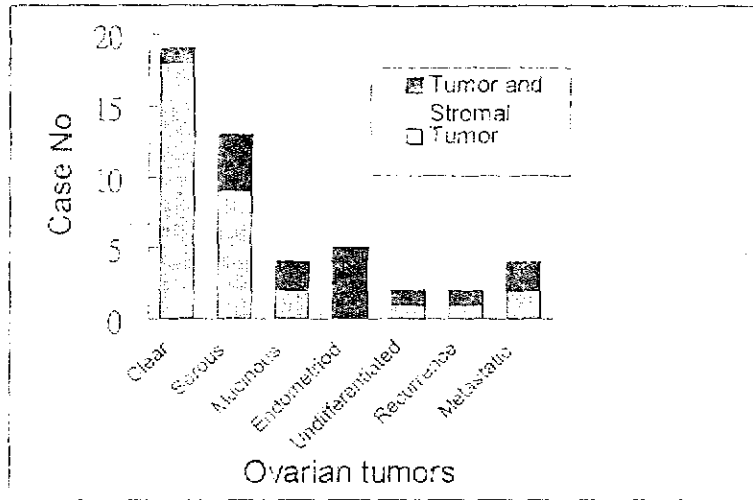


Fig 5. MMP-2 protein and mRNA distribution between tumor and stromal tissues in OCCA and non-OCCAs.

3. MMP activities in ovarian tumors.

The activities of MMPs in the ovarian tumors were analyzed by zymography. The MMP-9 activities were seen in all ovarian adenocarcinoma. But active MMP-2 was seen in all ovarian adenocarcinoma except clear cell carcinoma (Fig 6 and 7).

4. MMP activities in ovarian cancer cell line OVTW59 with different invasive capabilities.

The invasive difference (Fig 8), MMP-2 activities (zymography) (Fig9), and tumor growth during heterotransplantation (Fig 10) was previously reported. Tumors from the P0 and P4 heterotransplanted tumors were studied by zymography. Active MMP2 were seen in both P0 and P4 tumors. Latent MMP9 was seen in both tumor, however, only active MMP-9 was seen in P0 (Fig 11).

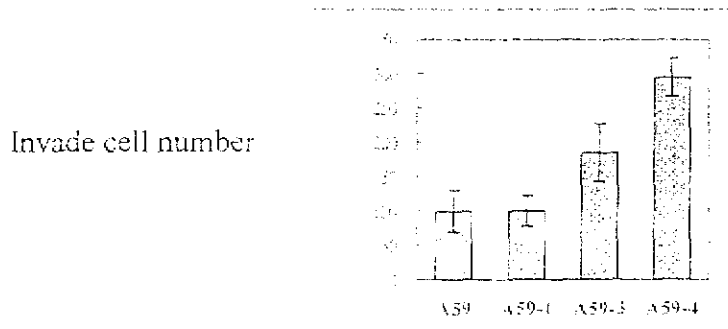


Fig 8. Subclones of ovarian carcinoma cell line (A59=P0, A59-1=P1, A59-3=P3, A59-4=P4) selected from Transwell Invasive Chamber, showing increasing invasion in in-vitro invasion assay.

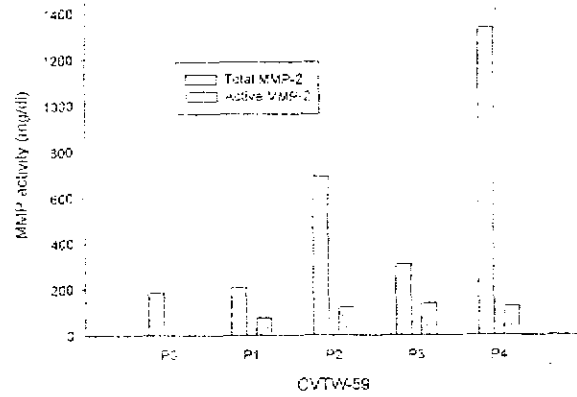


Fig 9. ELISA study showing P0 to P4 cells with increasing MMP2 activities (both latent and active forms).

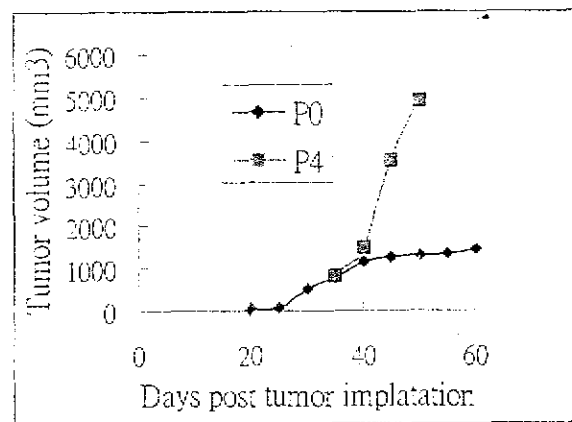


Fig 10 Tumor transplantation to scid mice showing greater tumor volume in tumor obtained from P4 cells then from P0 cells.

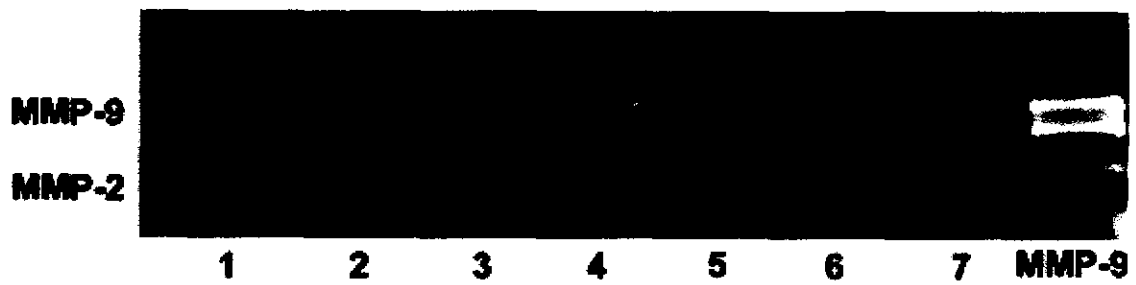


Fig 6. MMP activities of ovarian tumors showed in zymography. Lane 1 and 2: serous papillary adenocarcinoma, lane 3,4, 6: clear cell carcinoma, lane 5: metastatic tumor from breast cancer, lane 7: undifferentiated ovarian carcinoma.

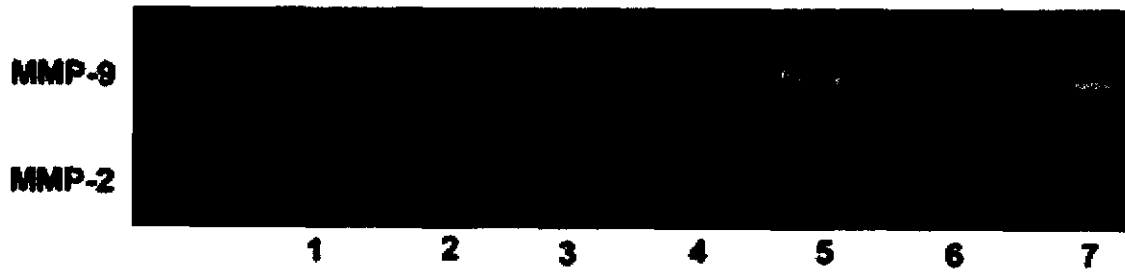


Fig 7. MMP activities of ovarian tumors showed in zymography. Lane 1: endometriod adenocarcinoma, lane2: metastatic, lane 3,4: serous papillary adenocarcinoma, lane5-7 clear cell carcinoma.



Fig 11. MMP activities of endometrial ovarian adenocarcinoma cell line OVTW59P0, and its subclone P4 showed in zymography.

Discussion:

The expression of MMP-2 and TIMP-2 was found uniquely expressed in the tumor cells of OCCA. In the other non-OCCAs, MMP-2 was found expressed both in tumor and stromal cells, especially in the stromal cells of serous papillary and mucinous cystadenocarcinoma. Expression of TIMP-2 was weaker in more advanced tumor and nearly co-localized with MMP-2 expression. By zymography, we further found that there were no active collagenase activities in OCCAs. From the zymography of ovarian tumors and ovarian cell line OVTW50 heterotransplantation, we found no values in the expression and activities of MMP-9 in tumor invasion.

Expression of MMP2 in ovarian tumor cells was reported to be due to the phenotypic plasticity of ovarian surface epithelial cells, i.e. the expression of both stromal and epithelial characteristics which may be a consequence of their mesodermal origin and their close developmental relationship with ovarian stromal fibroblasts (2).

MMP-2 is released in a pro-form and the stepwise cell surface activation of pro-MMP-2 is not clear (35). It was reported that MMP-2 is up-taken to the cell surface by a high-affinity receptor, and then followed by local activation by membrane-bound metalloproteinases, MT-MMP (36-38). It is still unclear if the binding and activation are through a common mechanism (36). Recently, it was reported that vitronectin receptor, the integrin $\alpha v \beta 3$, promotes maturation of MMP-2 in breast cancer cells (39). It was found colocalized with MMPs (40), especially at the invasive peripheral extremities of migrating cell invadopodia. The unique pattern of MMP-2 in OCCA from non-OCCA suggested a possible difference in the stepwise surface activation of MMP-2, that may be due to the different pathological entities. And it also suggested that activation of MMP-2 required its protein expression in the stromal cells.

The OCCA has been reported to be unique from other non-OCCA in the lower expression of mutant P53 (41), overexpression of MDM2 (42), and higher cell cycle regulating molecules (P21, cyclin E) (41). Structurally, the basement membrane material of OCCA was found to be more stromal hyalinization, which are immunoreactive for type IV collagen and laminin (43). This added to our evidence of the inactivation of the collagenase activities of MMP-2. Basement disruption was reported to be an early invasive and expression of type IV collagen in serous tumor (44). The unique incapability of collagenase activities of OCCA may therefore, causing it to be found at greater tumor size and early staging. It is yet unknown if this unique pattern of MMP

has any relationship to its higher incidence of endometriosis and deep vein thrombosis. Further studies will be focused in this part of phenomenon.

References:

1. Russel P. Surface epithelial-stromal tumors of the ovary. In: Kurman RJ. Blaustein's pathology of the female genital tract. 4th edition. New York: Springer-Verlag, 1994:705-82.
2. Afzal S, Lalani EN, Poulsom R, Stubbs A, Rowlinson G, Sato H, Seiki M, Stamp GWH. MT1-MMP and MMP-2 mRNA expression in human ovarian tumors: possible implications for the role of desmoplastic fibroblasts. *Hum Path* 1998;29:155-65.
3. Sasak CL, Fahey MT, Sakamoto A, Sato S, Tanaka T. Prognosis value of nuclear morphometry in patients with TNM stage T1 ovarian clear cell adenocarcinoma. *Br J Cancer* 1999;79:1736-41.
4. Serov SF, Scully RE, Sobin LH. International histologic classification of tumors, No 9. Histologic typing of ovarian tumors. Geneva, World Health Organization, 1973.
5. Kennedy AW, Biscotti CV, Hart WR, Webster KD. Ovarian clear cell adenocarcinoma. *Gynecol Oncol* 1989;32:342-9.
6. Goff BA, Sainz de la Cuesta R, Muntz HG, Fleishbacker D, Ek M, Rice LW, et al. Clear cell carcinoma of the ovary: a distinct histologic type with poor prognosis and resistance to platinum-based chemotherapy in stage III disease. *Gynecol Oncol* 1996;60:412-7.
7. Sakuragi N, Yamada H, Oikawa M, Okuyama K, Fujino T, Sagawa T, Fujimoto S. Prognostic significance of lymph node metastasis and clear cell histology in ovarian carcinoma limited to the pelvic (pT1M0 and pT2M0) *Gynecol Oncol* 2000;79:251-5.
8. Sugiyama T, Kamura T, Kigawa J, Terakawa N, Kikuchi Y, Kita T, Suzuki M, Sato I, Taguchi K. Clinical characteristics of clear cell carcinoma of the ovary. A distinct histologic type with poor prognosis and resistance to platinum based chemotherapy. *Cancer* 2000;88:2584-9.
9. Kennedy AW, Markman M, Biscotti CV, Emery JD, Rybicki LA. Survival probability in ovarian clear cell adenocarcinoma. *Gynecol Oncol* 1999;74:108-14.
10. Aure JC, Hoeg K, Kolstad P. Mesonephroid tumors of the ovary: clinical and histopathologic studies. *Obstet Gynecol* 1971;37:860-7.
11. Woessner JF. Matrix metalloproteinase and their inhibitors in connective tissue remodeling. *FASEB J* 1991;5:2145-54.